Microelectronics Reliability 98 (2019) 49–55

Contents lists available at ScienceDirect

Microelectronics Reliability

journal homepage: www.elsevier.com/locate/microrel

Residual stress and warpage of AMB ceramic substrate studied by finite element simulations

Shanshan Zhang[a], Huisheng Yang[a,*], Kewei Gao[a], Luchun Yan[a], Xiaolu Pang[a], Alex A. Volinsky[b]

[a] School of Materials Science and Engineering, University of Science and Technology Beijing, Beijing 100083, PR China
[b] Department of Mechanical Engineering, University of South Florida, Tampa, FL 33620, USA

ARTICLE INFO

Keywords:
Ceramic substrate
AMB
Residual stress
Warpage deformation
Finite element simulations

ABSTRACT

Ceramic substrates with high heat dissipation performance are utilized in high power electronic devices. This study investigates the warpage deformation and residual stress originating during manufacturing of the active material brazing (AMB) ceramic substrate to provide important parameters for the substrate design and ensure good reliability. Finite elements were used to analyze the effects of ceramic, metal and solder thickness, ceramic substrate size and pressure on residual stress distribution and warpage deformation. Calculation results of thermal elastic and thermal elastic-plastic finite elements are compared. Plastic deformation during the welding process greatly affects calculation results accuracy. It is found that the maximum axial stress is concentrated on the ceramic side and axial residual stress is the main factor causing cracking of the ceramic substrate. The thickness of ceramic, metal and solder, along with the substrate size have significant effects on residual stress and warpage deformation, which both can be reduced by applying external pressure.

1. Introduction

Compared with traditional plastic-based printed circuit board substrate, ceramic substrate has better thermal conductivity. Ceramic substrate combined with thicker metal layer can be used in high power electronic devices operating in extreme environments. Commonly used ceramic materials are AlN, Al_2O_3 and Si_3N_4 [1]. AlN substrate with high thermal conductivity of 170 W/mK provides a good alternative to conventional aluminum oxide (Al_2O_3) substrate with 24 W/mK for better heat dissipation. However, AlN substrate (α = 4.3 ppm/°C) still suffers from high thermal expansion coefficient (CTE) mismatch with copper (α = 16.3 ppm/°C) [2]. Active material brazing (AMB) ceramic substrate is a further development of direct bonded cooper (DBC), which is based on the reaction of ceramic and active elements at high temperature. Therefore, AMB ceramic substrate has higher binding force and reliability.

Residual stress arises at the ceramic/metal interface during cooling due to the CTE mismatch. The value of residual stress is affected by many factors. Residual stress has a great effect on the ceramic/metal interface performance. Larger deformation leads to reduced etching precision, while higher residual stress reduces fatigue resistance and service lifetime. Therefore, it is of great importance to control substrate deformation and reduce residual stress to improve precision and service performance.

The most common method to determine thin film residual stress is based on the substrate bending deformation in terms of the substrate radius of curvature. Residual stress in thin film can be calculated using the Stoney Eq. (3):

$$\sigma_f = \left(\frac{E_s}{1-\gamma_s}\right)\frac{t_s^2}{6rt_f} \tag{1}$$

Here, E_s and γ_s are the Young's modulus and Poisson's ratio of the substrate material. t_s and t_f represent the thickness of the substrate and the film, respectively. One of the accuracy conditions for this formula is that the film is much thinner than the substrate. However, in this paper, metal layer thickness is relatively close to the thickness of the ceramic substrate, and plastic deformation occurs in metal during cooling. When the thickness of the substrate is close to the film, or the structure under the action of residual stress has large deformation, accuracy of the residual stress results will be affected. Here, residual stress is calculated using the finite element method (FEM) in order to ensure accuracy of the results.

Since the thickness of the material is variable, the radius of curvature should not be used to measure the stress at the interface. Thermal residual stress can be expressed using Eq. (2) [4], which doesn't take into account material thickness:

* Corresponding author.
E-mail address: hsyang@263.net (H. Yang).

https://doi.org/10.1016/j.microrel.2019.04.025
Received 8 February 2018; Accepted 29 April 2019

$$\sigma_m = \sigma_c = \left[1/\left(\frac{1}{E_m} + \frac{1}{E_c}\right)\right](\alpha_m - \alpha_c)\Delta T \tag{2}$$

Here, E_m is the elastic modulus of metal, E_c is the elastic modulus of ceramics, α_m is the thermal expansion coefficient of metal, α_c is the thermal expansion coefficient of ceramics, and ΔT is the cooling interval from high to low. This formula only calculates thermal residual stress of the joints in the elastic range, and does not take into account variations of material properties with temperature, so there is a large deviation in calculation results.

The finite element method has been widely used to predict residual stresses in brazed joints. However, the research on residual stress and deformation of AMB ceramic substrate has not been reported yet. Gong et al. [5] analyzed the factors affecting residual stress of stainless steel plate-fin structure using finite element analysis. The results showed that material mismatch, brazing gap, pressure loading, fin pitch, thickness and height, along with the plate thickness significantly affect residual stress distribution. Wang et al. [8] investigated thermal stress distribution of the Si_3N_4/42CrMo joints brazed with the TiNp modified active filler. The results indicated that the peak tensile axial residual stresses always emerged in the Si_3N_4 ceramics. There have been many articles to study the stress variation of the DBC ceramic substrate under cyclic heating conditions [6,7]. Tsai et al. [2] conducted a finite element study of the direct plated copper (DPC) aluminum nitride (AlN) substrate. It is also found from the validated finite element simulation that the Cu-film wedge angle, length, and thickness significantly affect the maximum 1st principal stress of AlN during thermal cyclic loading.

In this paper, the effects of ceramic, metal and solder thicknesses, along with ceramic substrate size and pressure on residual stress and warpage deformation generated in brazing process are analyzed by means of the finite element analysis. This study is helpful to control the residual stress and deformation in the production process. At present, the calculation of the residual stress and deformation is usually realized by numerical simulations. In the simulation process, ceramic substrate can be warped freely without mechanical constraints. The purpose of this study is to understand the mechanism of the residual thermal stress forming in ceramic substrate and to grasp the law of deformation and the main influencing factors. At last, calculation results are discussed in detail. The research conclusions provide theoretical and practical guidance for the production process.

2. Finite element model

Based on the thermal elastoplastic stress strain behavior and considering materials' properties change with temperature, ANSYS was used to analyze residual stress and deformation of AMB ceramic substrates. The model is a single surface ceramic substrate, shown in Fig. 1. The sample was cooled to room temperature from 800 °C at 10 °C/min cooling rate. The reaction layer was not taken into consideration in the analysis because it was too thin and the effects of phase changes were ignored. It was assumed that the sample temperature during cooling was homogeneous with perfect interfacial adhesion. In addition, the effects of interfacial reinforcement were not considered in calculations. The von-Mises yield criterion was adopted and the equivalent stress is [7]:

$$\bar{\sigma} = \left\{\frac{1}{2}[(\sigma_x - \sigma_y)^2 + (\sigma_y - \sigma_z)^2] + 3(\tau_{xy}^2 + \tau_{yz}^2 + \tau_{zx}^2)\right\}^{\frac{1}{2}} \tag{3}$$

The model was analyzed by the 3D elastic-plastic finite element method. The model was meshed using the 8-nodes. In the simulation process, the constraints imposed on the model are shown in Fig. 2. The sample and the rigid base were set as a contact pair, so that the sample can warped freely. 1/4 symmetry models were adopted to simplify the finite element calculations.

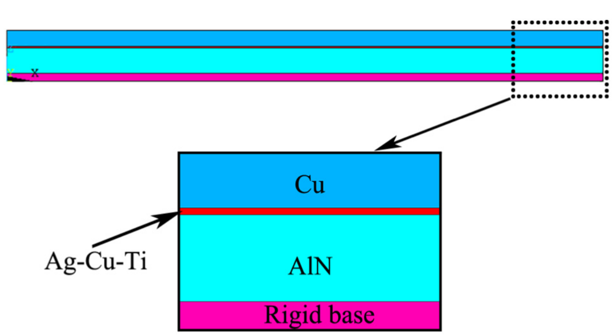

Fig. 1. Cross-section of the FEM model.

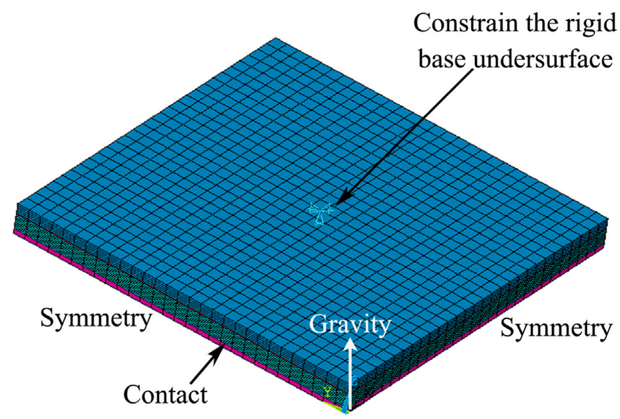

Fig. 2. Finite elements mesh and load of the ceramic substrate.

3. Results

3.1. Comparison of thermal elastic and thermoplastic finite elements

In this paper, calculation results of thermal elastic finite elements and thermal elastic-plastic FEM are compared, and the results calculated by thermal elastic-plastic FEM are closer to the actual measurement results. In this model, the thickness of the ceramic is 0.635 mm, the thickness of the copper metal layer is 0.3 mm and the thickness of the Ag-Cu-Ti solder layer is 50 μm. The deformation of the sample was measured with the digimatic height gage, shown in Fig. 3. If plastic deformation of the welding process is not considered, the reliability of the calculation will be greatly reduced. However, the calculation results of the thermal elastic-plastic FEM can be better suited to the actual

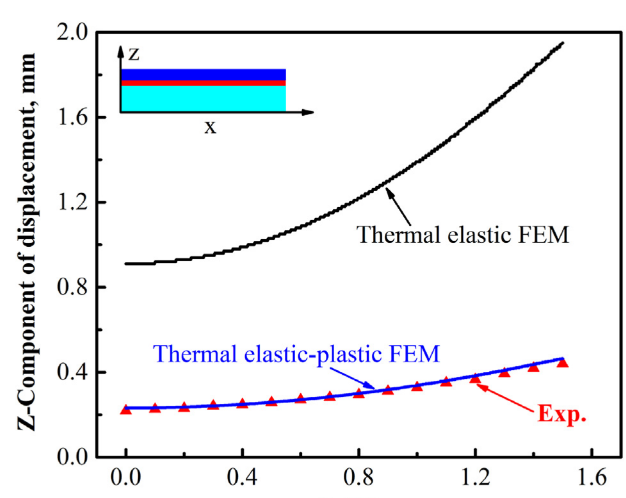

Fig. 3. Warping deformation of the single side welded AlN ceramic substrate, cooled to room temperature from 800 °C at 10 °C/min cooling rate.

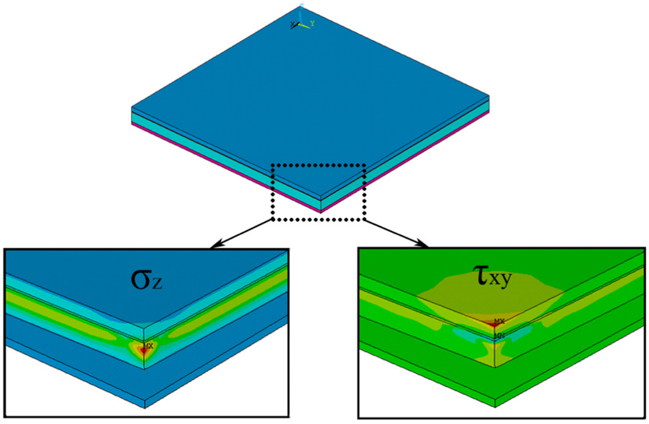

Fig. 4. Shear stress and axial residual stress maps in the sample corner region.

situation and the calculations are reliable. According to the results of the shear stress calculations and axial residual stress maps of the samples in the corner region of Fig. 4, it can be seen that the axial tensile stress is the main factor for the failure of the ceramic substrate.

3.2. Ceramics thickness effects on warpage and residual stress

Axial residual stress and warpage deformation are not only affected by the thermal expansion coefficients of the materials, but also the size of the substrate. Finite element models with different ceramic thickness were simulated to reveal the effects of the ceramic thickness on warpage deformation and residual stress. The thickness of copper film was 0.3 mm and the Ag-Cu-Ti filler metal layer was 50 μm and the area of the ceramic substrate remained the same. The axial residual stress and warpage deformation maps of ceramic substrate with thickness of 0.635 mm are shown in Fig. 5(a) and Fig. 5(b). From the axial residual stress maps, the maximum axial stress is concentrated on the ceramic side. Distribution of the σ_z along the PQ path for different ceramic thicknesses is shown in Fig. 6(a). It can be seen that the ceramic thickness variation had a great impact on maximum σ_z. When the thickness of ceramic increases, the residual stress distribution remains basically unchanged, but the peak stress increases. It is obvious that the greater the ceramic thickness, the greater the axial stress is. In addition, it can be seen that the axial stress is tensile. Fig. 6(b) shows the relationship between the ceramic thickness and the *Z*-component of the displacement along the MN path. Note that X is defined as the length from M to N, indicating that with the increasing ceramic thickness, the overall warping gradually decreases. From Fig. 6(a) and Fig. 6(b), the maximum axial residual stress corresponding to the ceramic thickness of 0.3 mm, 0.5 mm, 0.635 mm and 1 mm is 161 MPa, 215 MPa, 239 MPa and 278 MPa, respectively. The maximum axial displacement corresponding to ceramic thickness of 0.3 mm, 0.5 mm, 0.635 mm and 1 mm is 3.165 mm, 1.47 mm, 0.922 mm and 0.376 mm, respectively. When the ceramic thickness is 0.3 mm, the deformation is the maximum, and the axial stress of the corresponding ceramic substrate is the minimum.

3.3. Cooper layer thickness effects on warpage and residual stress

Copper layer thickness of the ceramic substrates is a vital parameter, which is important for warpage deformation and axial residual stress development. In order to investigate the cooper layer thickness effects, four FEM models with 0.1 mm, 0.2 mm, 0.3 mm and 0.4 mm cooper thickness were developed. The axial residual stress distribution along the PQ path and Z-component of displacement along the MN path of ceramic substrate with different copper layer thickness are shown in Fig. 7(a) and Fig. 7(b). It is shown that the axial residual stress increases with cooper thickness. The maximum axial residual stresses corresponding to the cooper layer thickness of 0.1 mm, 0.2 mm, 0.3 mm and 0.4 mm is 140 MPa, 200 MPa, 239 MPa and 271 MPa, respectively. The maximum axial displacement corresponding to the cooper layer thickness of 0.1 mm, 0.2 mm, 0.3 mm and 0.4 mm is 0.207 mm, 0.626 mm, 0.922 mm and 1.277 mm, respectively. For the 0.1 mm thick cooper layer, the deformation gradient of the ceramic substrate is very small, which decreases residual stress. With the metal thickness increase, the overall trend of residual axial stress along the PQ path did not change significantly, but the stress peak value increased.

3.4. Solder thickness effects on warpage and residual stress

In this section, four models were designed to study the effects of the solder layer thickness on warpage deformation and residual stress of AMB ceramic substrate: 30 μm, 50 μm, 70 μm and 100 μm. Solder layer thickness effects on axial stress along the PQ path and the *Z*-component of displacement along the MN path are shown in Fig. 8. The axial stress increases with the solder layer thickness. The maximum axial residual stresses corresponding to the solder thickness of 30 μm, 50 μm, 70 μm and 100 μm is 229 MPa, 239 MPa, 253 MPa and 278 MPa, respectively. The maximum axial displacement corresponding to the solder thickness of 30 μm, 50 μm, 70 μm and 100 μm is 0.826 mm, 0.922 mm, 1.026 mm and 1.193 mm, respectively.

3.5. Substrate size effects on warpage and residual stress

Similar analysis was performed by considering the size of the substrate, as shown in Fig. 9. When the size of substrate increases from 1 × 1 cm to 2 × 2 cm and to 3 × 3 cm, the warpage deformation increases. However, the axial residual stress decreases with increasing substrate size. The maximum axial residual stress corresponding of 1 × 1 cm, 2 × 2 cm and 3 × 3 cm size is 436 MPa, 350 MPa and 239 MPa, respectively. The maximum axial displacement corresponding to 1 × 1 cm, 2 × 2 cm and 3 × 3 cm size is 0.114 mm, 0.377 mm and 0.922 mm, respectively. With the sample size decrease, the trend of

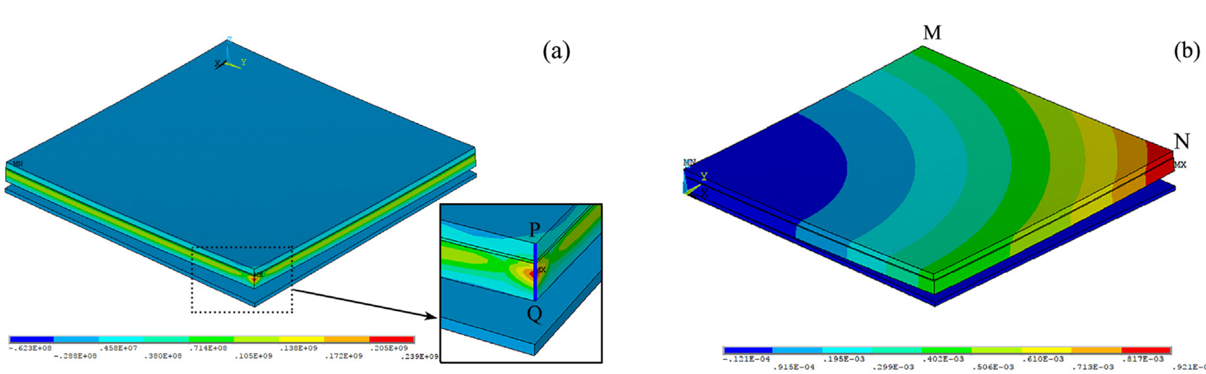

Fig. 5. Simulation results of the 0.635 mm thick ceramic substrate with 50 μm metal: (a) σ_z; (b) *Z*-component displacement.

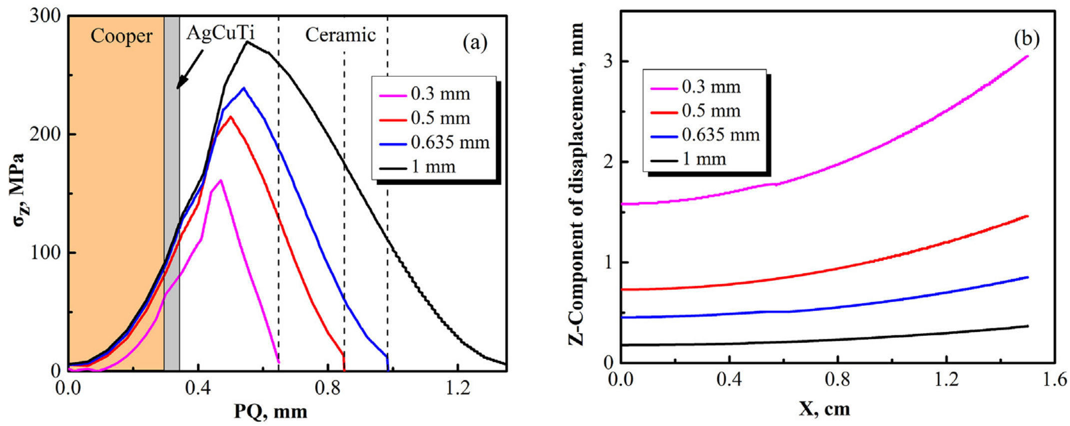

Fig. 6. (a) Distributions of σ_z along the PQ path for different thickness ceramics; (b) Z-component of the displacement along the MN path.

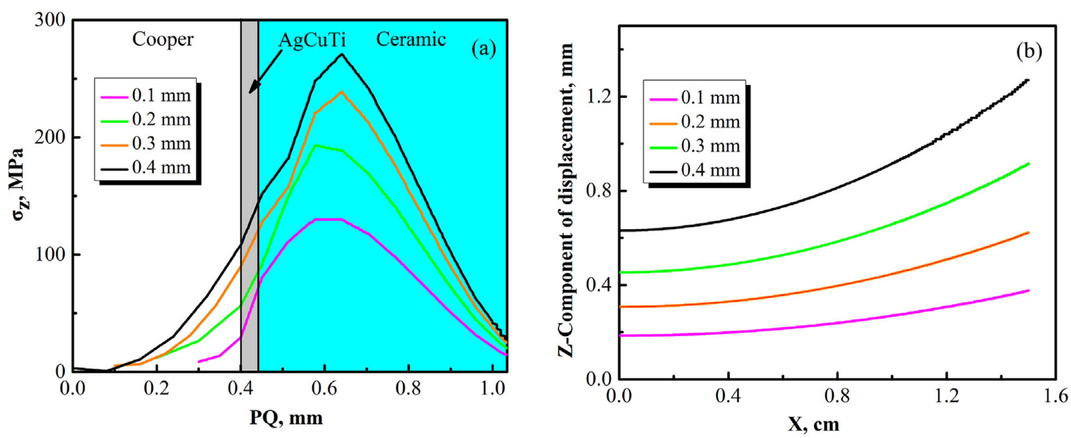

Fig. 7. (a) Distributions of σ_z along the PQ path for different thickness of cooper layer; (b) *Z*-component of displacement along the MN path.

residual stress distribution has changed. For the 1 cm × 1 cm sample, the distribution of axial residual stress along the PQ path is not completely tensile, which changes from tensile to compressive further from the interface.

3.6. Pressure effects on warpage deformation and residual stress

The generation of thermal stress is a process of accumulation, the axial residual stress and warpage deformation of the interface can be reduced by applying certain pressure on ceramic substrate during brazing process, the results are shown in Fig. 9. With the increase of brazing pressure, the distribution trend of axial residual stresses is basically unchanged, but the greater the applied pressure, the more the axial residual stress of the interface is released. When pressure is 1 MPa, the stress at the interface is the same as with no pressure applied. However, at 10 MPa substrate pressure, the axial residual stress is reduced to 227 MPa. At the same time, pressure should not be excessive, otherwise it will cause ceramic fracture and solder overflow. Fig. 10(a) shows σ_z distribution along the PQ path for different pressure applied to the substrate. Fig. 10(b) shows the *Z*-component displacement along the MN path and Fig. 10(c) shows the magnified area.

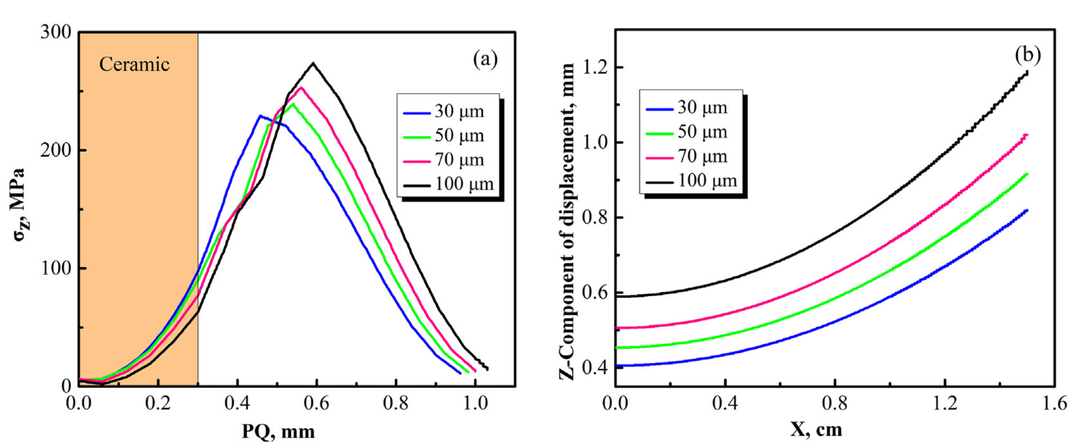

Fig. 8. (a) Distribution of σ_z along the PQ path for different solder layer thickness; (b) Z-component of displacement along the MN path.

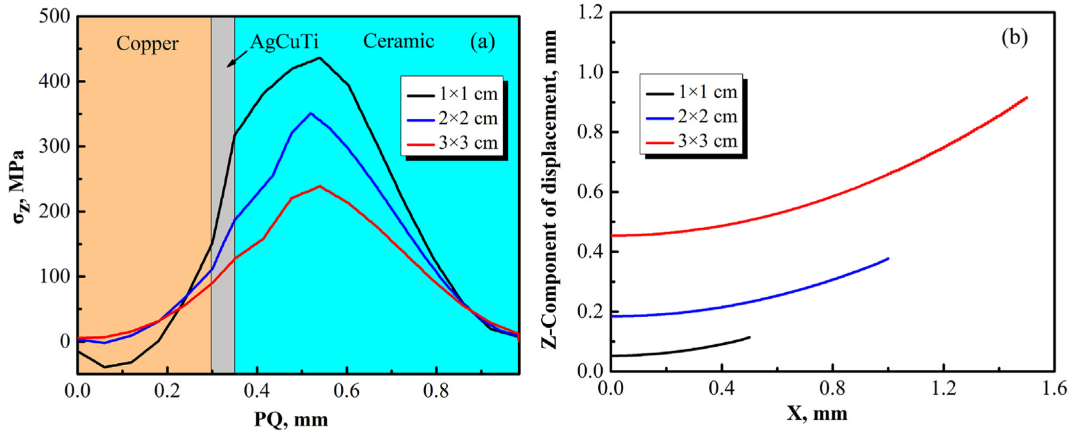

Fig. 9. (a) Distribution of σ_z along the PQ path for the different size substrate; (b) *Z*-component of displacement along the MN path.

4. Discussion

Since the thermal expansion coefficient of the ceramic substrate is not matched, warping occurred during the substrate cooling process [7]. Ceramic materials can have similar elastic properties as metals. However, since the atoms in ceramics are covalently bonded, it is harder to plastically deform ceramics compared to metals. Due to the high brittleness of ceramic materials, there's minimal plastic deformation at room temperature. Metals can easy slip and produce plastic deformation due to the lack of metal bonds directionality. Ceramic materials are often formed by covalent and ionic bonds, and covalent bonds obviously have directionality, so a smaller number of slip systems exists in ceramic materials. Therefore, most ceramics can hardly produce plastic deformation at room temperature, which is the main characteristic of ceramic mechanical behavior. With the increase of temperature and the extended time, some ceramic materials can show certain ability for plastic deformation. Plastic deformation of ceramics is mainly in the form of creep [8–11]. Plastic deformation ability of ceramic is poor, so stress concentrations are easily generated. Tensile strength of aluminum nitride is 270 MPa [3]. Therefore, the stress in ceramics should not exceed this value. Ceramic substrate failure is mainly manifested by the lateral fracture of the ceramic side [12].

This study also studied the influence of ceramics and metal sizes on axial residual stress and warpage deformation of the interface. The

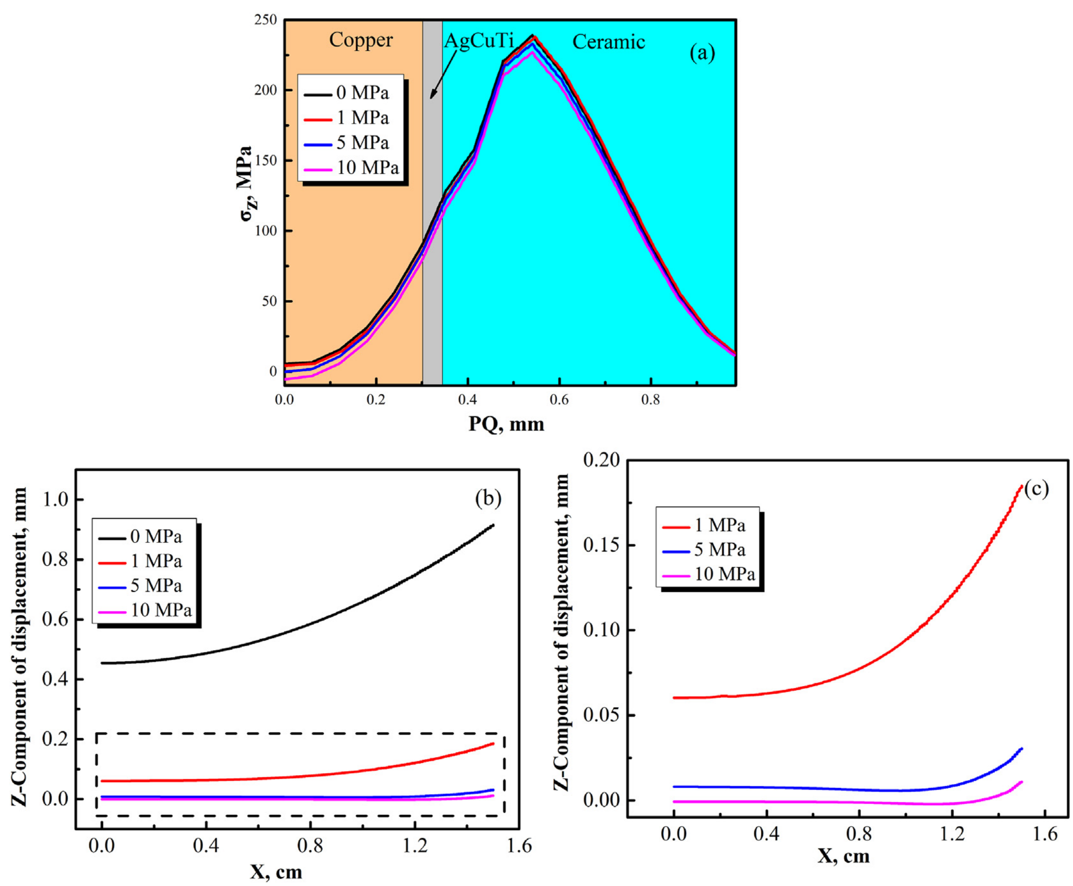

Fig. 10. (a) Distributions of σ_z along the PQ path for different pressure applied to the substrate; (b) Z-component of displacement along the MN path and (c) magnified area.

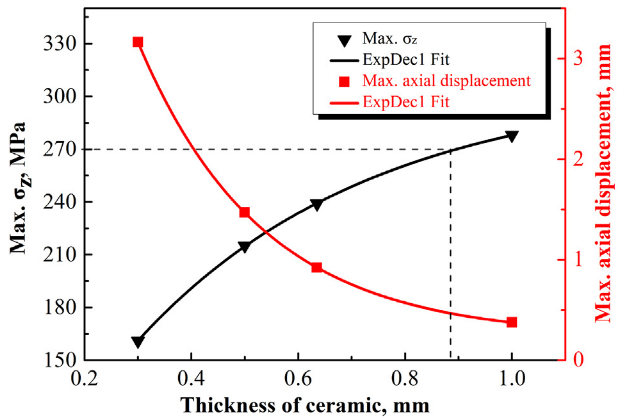

Fig. 11. Maximum axial residual stress and maximum warpage deformation curves for the thickness of ceramics varied from 0.3 mm to 1 mm.

results presented here show that the thickness of ceramic has a fundamental effect on the ceramic substrates behavior. The maximum axial residual stress and maximum warpage deformation curves along with the thickness of ceramics varied from 0.3 mm to 1 mm are shown in Fig. 11. The dotted line indicates that the tensile strength of the ceramics is 270 MPa. If the axial residual stress exceeds this value, ceramics would crack. It can be seen that the maximum axial deformation and the maximum axial stress both have exponential relationship with ceramic thickness. However, the maximum axial stress increases with ceramic thickness, while the maximum axial deformation decreases with ceramic thickness. Due to the increase of ceramic thickness, the overall stiffness of ceramic substrate is increased.

As shown in Fig. 12, the axial residual stress and the axial maximum deformation increase with the metal thickness. Due to the increased metal thickness, more plastic deformation will occur during the cooling process, resulting in larger warpage of the substrate. When the metal layer is too thick, it can cause a lot of shrinkage, resulting in higher residual stress at the interface, which can cause ceramics fracture.

Fig. 13 shows the maximum axial stress and the maximum axial displacement change with increasing solder thickness. It can be seen that the maximum axial stress increases exponentially with the solder thickness. Similar to the copper layer, the maximum axial displacement is linear with the solder thickness. The solder thickness needs to be optimized for the brazing process. If solder is too thick, large axial residual stress can be produced at the interface, which can cause cracking of ceramic substrates. On the contrary, if the solder layer is too thin, the interface bond strength would be decreased.

Three different ceramic substrate sizes were designed in this study,

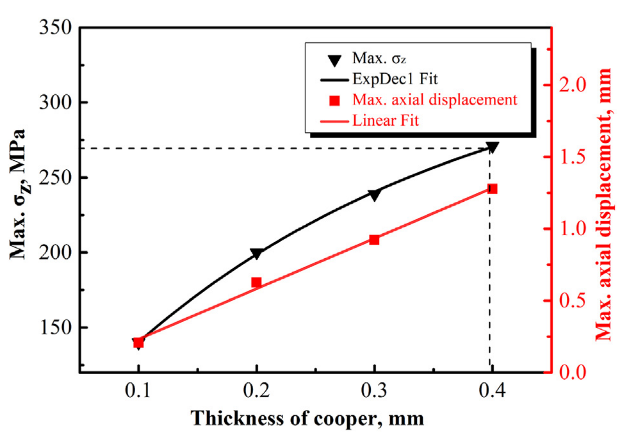

Fig. 12. Maximum axial residual stress and maximum warpage deformation curves along with the thickness of cooper varied from 0.1 mm to 0.3 mm.

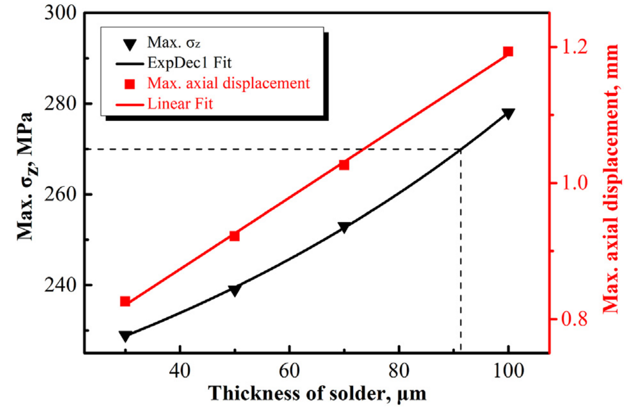

Fig. 13. Maximum axial residual stress and maximum warpage deformation curves along with the thickness of solder varied from 30 μm to 100 μm.

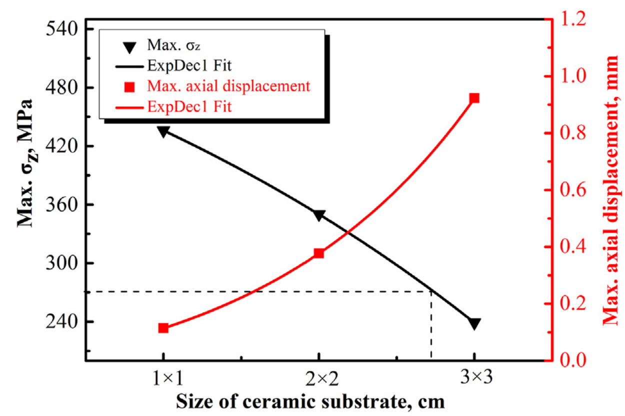

Fig. 14. Maximum axial residual stress and maximum warpage deformation curves along with the 1 × 1 cm, 2 × 2 cm and 3 × 3 cm substrate size.

1 × 1 cm, 2 × 2 cm and 3 × 3 cm, respectively. Ceramic substrate size effects on maximum axial residual stress and maximum warpage deformation are shown in Fig. 14. It is found that the larger the size of the ceramic substrate, the smaller the maximum axial residual stress, but the deformation keeps increasing.

When the pressure on the ceramic substrate increases continuously, the axial residual stress and warping deformation decrease, as shown in Fig. 15. It can be seen that as the pressure is increased, deformation tends to stabilize. However, axial residual stress decreases at higher pressure due to the fact that applying pressure can disperse stress.

The double-sided brazed sample model was also simulated in this

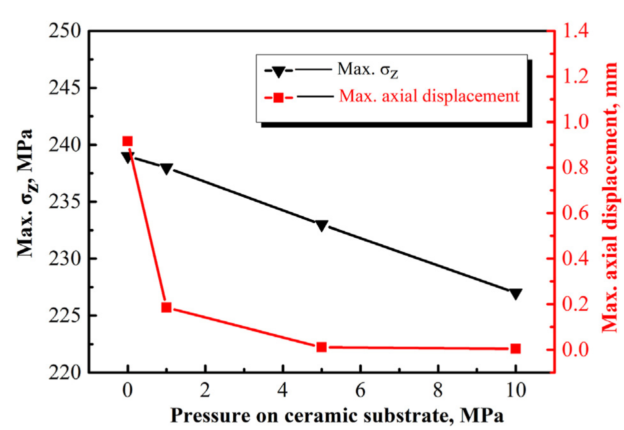

Fig. 15. Maximum axial residual stress and maximum warpage deformation curves along with the pressure varied from 0 MPa to 10 MPa.

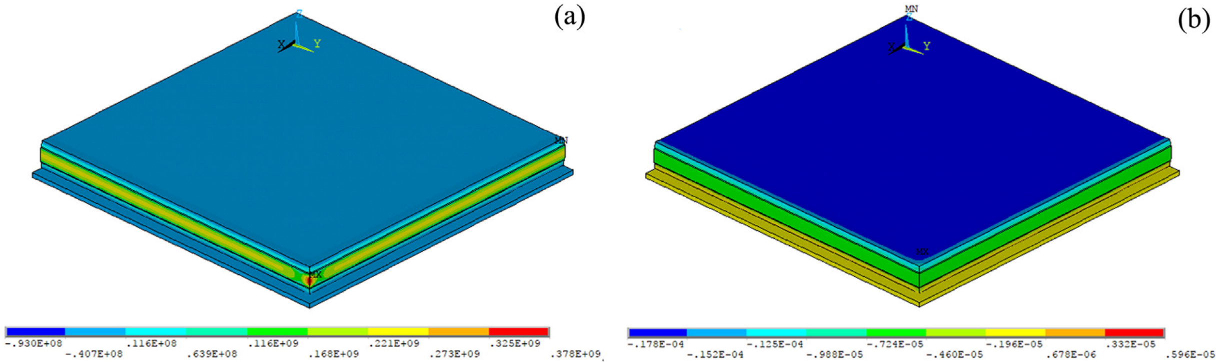

Fig. 16. Double-sided brazed ceramic substrate: (a) σ_z and (b) *Z*-component of the displacement.

study. The results of the axial residual stress and warpage deformation maps are shown in Fig. 16. It is seen that the warpage deformation of the double-sided brazed samples can be reduced, but the axial residual stress increases in ceramics. Since the axial residual stress and deformation of the two sides of the metals are opposite, the warpage deformation can be offset, but the axial residual stress will increase to 378 MPa. In the brazing process, pressure should be applied to the sample to reduce the stress concentration on the ceramic side.

Therefore, the effect of the above parameters on the residual stress should be taken into consideration in the process of making the AMB ceramic substrate. Through reasonable design, the residual stress of the substrate will be reduced and the service life of the product will be improved. It is also possible to use higher tensile strength silicon nitride ceramics, and the use of multi-layer middle layer or composite solder for future development of ceramic substrates.

5. Conclusions

In this study, axial residual stress and warpage deformation of AMB ceramic substrate during cooling process was studied. The increase of ceramic, metal and solder thickness and pressure have little effects on the trend of axial residual stress distribution within a certain range. However, there are significant effects on the maximum axial stress value. The maximum axial residual stress increases with ceramic substrate thickness, but warpage deformation decreases, gradually leveling off. The axial residual stress and warpage deformation increase with metal layer thickness. Different sizes of samples were also studied. Larger substrate area results in larger deformation and smaller axial residual stress. Higher pressure during the cooling process reduces axial residual stress and warpage deformation of the substrate. The maximum axial stress is on the ceramic side, and the axial stress is tensile. However, as the size of the substrate decreases, the axial residual stress increases, without changing residual stress distribution trend. Compressive stress occurs along the PQ path when the sample is small enough. The axial stress of the double-sided ceramic substrate was increased, but the warpage deformation decreased. This study provides guidance for better ceramic substrate system design.

Acknowledgements

This work was supported by the National Key Research and Development Program of China (No. 2016YFB0700201).

References

[1] H. Miyazakia, S. Iwakiri, K. Hirao, S. Fukuda, N. Izu, Y.I. Yoshizawa, H. Hyuga, Effect of high temperature cycling on both crack formation in ceramics and delamination of copper layers in silicon nitride active metal brazing substrates, Ceram. Int. 43 (6) (2017) 5080–5088.
[2] M.Y. Tsai, P.S. Huang, C.H. Lin, C.T. Wu, S.C. Hu, Mechanical design and analysis of direct-plated-copper aluminum nitride substrates for enhancing thermal reliability, Microelectron. Reliab. 55 ((12) (2015) 2589–2595.
[3] Stoney G G, The tension of thin metallic film deposited by electroplating. Proc. R. Soc. Med., (82) (1909) 172.
[4] Y.H. Zhou, K. Ikeuchi, T.H. North, Z.R. Wang, Effect of plastic deformation on residual stresses in ceramic/metal interfaces, Metall. Trans. A. 22 (1991) 2822–2824.
[5] Jianming Gong, Wenchun Jiang, Qinshan Fan, Hu Chen, S.T. Tu, Finite element modelling of brazed residual stress and its influence factor analysis for stainless steel plate-fin structure, Int. J. Mater. Prod. Technol. 209 (2009) 1635–1643.
[6] L. Dupont, Z. Khatir, S. Lefebvre, S. Bontemp, Effects of metallization thickness of ceramic substrates on the reliability of power assemblies under high temperature cycling, Microelectron. Reliab. 46 (2006) 1766–1771.
[7] L. Xu, M.C. Wang, Y. Zhou, Z.F. Qian, S. Liu, An optimal structural design to improve the reliability of Al_2O_3–DBC substrates under thermal cycling, Microelectron. Reliab. 56 (2016) 101–108.
[8] R. Von Mises, Mechanik der festen köper im plastisch deformablen zustand, Nachrichten Der Gesellschaft Der Wissenschaften Göttingen Math Klasse, Göttingen, 1913, pp. 582–592.
[9] A.H. Chokshi, T.G. Nieh, J. Wadsworth, Role of concurrent cavitation in the fracture of a superplastic zirconia—alumina composite, J. Am. Chem. Soc. 74 (4) (1991) 77.
[10] H.J. Frost, M.F. Ashby, Deformation mechanism maps: the plasticity and creep of metals and ceramics, Pergamon Press, 1982, pp. 80–98.
[11] M. Sakai, R. Nowak, Fracture toughness and brittleness of ceramic materials, Ceramics. Adding the Value. 2 (1992) 922.
[12] Jean-Paul Poirier, Creep of Crystals: High-Temperature Deformation Processes in Metals, Ceramics and Minerals, Cambridge University Press, 1985.